Progress In Electromagnetics Research, PIER 60, 131–142, 2006

A RIGOROUS ANALYSIS AND EXPERIMENTAL RESEARCHES OF WAVEGUIDE MAGIC TEE AT W BAND

H. C. Wu and W. B. Dou

State Key Laboratory of Millimeter Waves
Southeast University
Nanjing 210096, China

Abstract—A waveguide magic tee at W band is analyzed exactly and developed. The analysis approach is a combination of the mode expansion method and finite element method, which is based on the weak form of Helmholtz equation. Mode expansion instead of PML (Perfectly Matched Layers) is used to truncate the computing space of finite element. A magic tee at W band (75∼110 GHz) with the structure, which is easy for manufacture, is developed. Calculated results are presented and compared to those in experiments. Agreement has been observed. A sensitivity analysis is carried out, which shows the influence of the tolerance of manufacture on the performance of the magic tee. And the power carrying capacity of the designed magic tee is also evaluated.

1. INTRODUCTION

Waveguide magic tee is an important element in microwave and millimeter wave engineering especially in monopulse antenna systems. However, because of the complicated structure and small size, good performance magic tees at millimeter wave wavelength such as at W band or higher frequencies is very difficult to realize. On the other hand, a rigorous field analysis on waveguide magic tee is also difficult. So far as we know only a little papers have been published on the analysis. Sieverding and Arndt analyzed the magic tee with the full wave modal S-matrix by mode-matching method in 1993 [1]. Later Ritter and Arnd presented a new method, named "a combined finite-difference time-domain/matrix-pencil method", to analyze and design magic tee [2]. In 2002, Shen et al. introduced another method, a hybrid finite-element/modal expansion method, for the rigorous analysis and

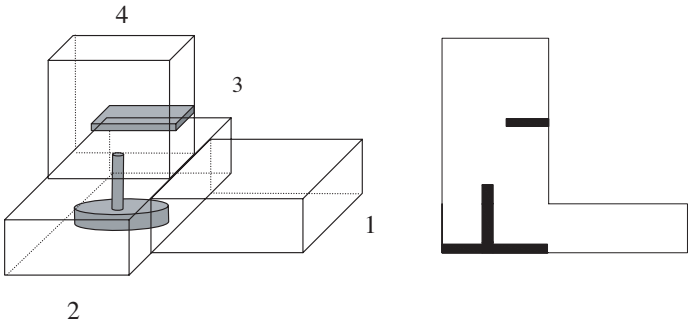

Figure 1. Schematic diagram of magic tee in Ref. [2].

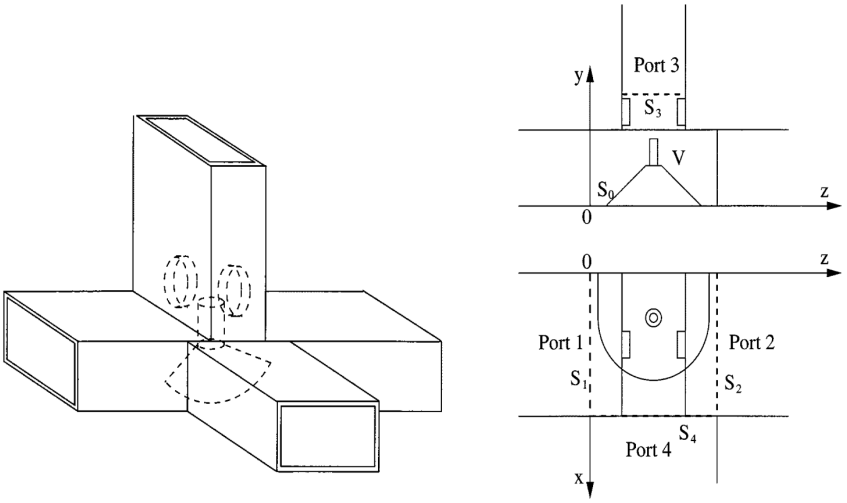

Figure 2. Schematic diagram of magic tee in Ref. [3].

design of a magic T-junction [3]. In 2003, the finite element/mode matching was applied by R. Beyer and U. Rosenberg to the design of magic tees [4]. However, the waveguide magic tees they designed are all limited to that at X band or Ku band. And in ref. [2] and [3], in order to get good performance, matching metal steps or metal plates are placed in port 4 of waveguide magic tee besides the matching element in magic tee junction (shown in Fig. 1 and Fig. 2). We use machine tool to manufacture the magic tee. In microwave band, because the size of waveguide is large, the matching metal steps or metal plates in port 4 of magic tee, as shown in Fig. 1 and Fig. 2, can be made accurately, and make the roughness as small as possible. However,

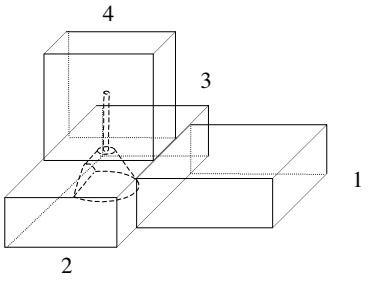

(a) Geometry of magic Tee in this paper

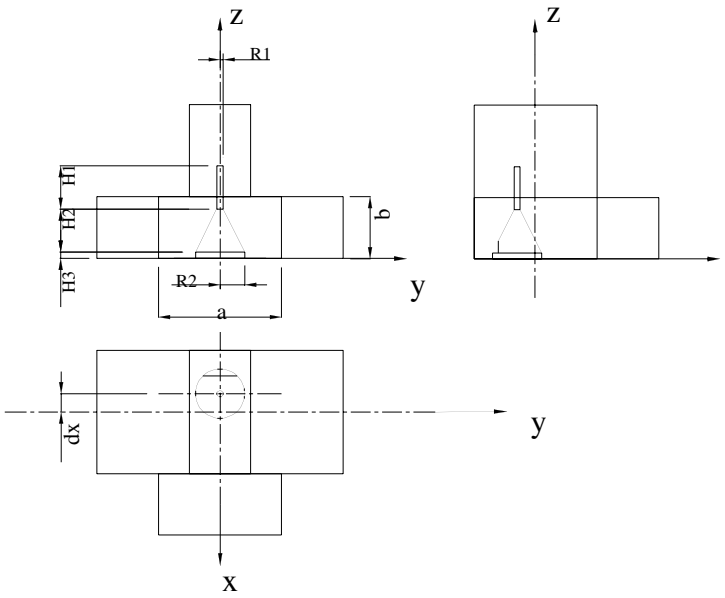

(b) Different view of Magic Tee

Figure 3. Schematic diagram of magic tee in this paper $a = 2.54,\ b = 1.27,\ dx = 0.15,\ R1 = 0.12,\ R2 = 0.9,\ H1 = 1.15,\ H2 = 0.3,\ H3 = 0.1\,(\mathrm{mm})$.

in W band it is very difficult to reach the requirement because of waveguide size only 2.54 mm*1.27 mm. To reduce the difficulty of manufacture, the matching elements in port 4 of magic tee shown in Fig. 1 and Fig. 2 are eliminated. So a waveguide magic tee with only one matching component in junction, which is similar to that as shown in Fig. 1 and Fig. 2, is obtained and depicted in Fig. 3. For this structure with only one matching element in the junction, the

matching element can be placed in the junction by inserting it into the junction through a hole in the bottom of junction, so it is easy to manufacture compare to the structure given in Fig. 1 and Fig. 2. This waveguide magic tee is analyzed and designed by an FEM approach based on Helmholtz equation weak form and mode expansion. The Helmholtz equation weak form was introduced by Peterson to analyze some two dimensional problems of electro- magnetic scattering from inhomogeneous cylinder [5]. Based on the weak form, a final set of linear equations have been acquired by using interpolation to present the electric field and magnetic field in the complicated structure, and combining the mode expansion in the regular region to truncate the computing region. Experimental researches are carried out after analysis and numerical computation. From the figures shown below, it can be seen that agreement has been observed between the calculation results and the measured results. And the performance of the magic tees is good and has met the requirement of the practical application. At last, the maximum E-fields in the magic tee for different ports input are calculated. According to this maximum E-field, the power carrying capacity of the designed magic tee is evaluated.

2. ANALYSIS APPROACH

The waveguide magic tee to be analyzed is shown in Fig. 3, which results from the magic tees of Figures 1 and 2. Four waveguide ports are joined to form an E-H tee and a matching element is placed in the tee junction to make it magic tee. The irregularly shaped matching element should be modeled with high precision. The fields are expressed with different functions at different regions.

In the junction:

$$\vec{E} = \sum_{n=1}^{N} A_n \vec{N}_n(x, y, z) \tag{1}$$

In the 1st waveguide (Port 1):

$$\vec{E} = e_{11}^{in}\vec{e}_{11}^{in}(x, y, z) + \sum_{l=1}^{L} e_{1l}^{s}\vec{e}_{1l}^{s}(x, y, z) \tag{2}$$

In the ith waveguide (Port i):

$$\vec{E} = \sum_{l=1}^{L} e_{il}^{s}\vec{e}_{il}^{s}(x, y, z) \qquad i = 2, 3, 4 \tag{3}$$

Where, $\vec{N}_n(x,y,z)$ denotes the first-order tetrahedral elements in vector finite element; A_n denotes the interpolated value of E at that vector; $\vec{e}_{il}(x,y,z)$ denotes electric vector eigenfunction of the lth mode in the ith waveguide; e_{il} denotes the coefficient of electric vector eigenfunction of the lth mode in the ith waveguide; and L denotes the number of the modes expended.

Substitute test function $\vec{T} = \vec{N}_i(x,y,z)\ \ i = 1,2,\ldots,N$ in Helmholtz weak form [6],

$$\iiint_I \left[\nabla\times\vec{N}_i\cdot\left(\overline{\overline{\mu}}_r^{-1}\nabla\times\sum_{n=1}^{N}A_n\vec{N}_n\right)-k^2\vec{N}_i\cdot\left(\overline{\overline{\varepsilon}}_r\sum_{n=1}^{N}A_n\vec{N}_n\right)\right]dV = -\sum_{j=1}^{3}\iint_{S_j}\vec{N}_i\cdot\left[\hat{n}\times\overline{\overline{\mu}}_r^{-1}(\nabla\times\vec{E})\right]dS \quad (4)$$

N equations can be obtained. Where

$$\overline{\overline{u}}_r=\begin{bmatrix}\mu_{xx}&\mu_{xy}&\mu_{xz}\\ \mu_{yx}&\mu_{yy}&\mu_{yz}\\ \mu_{zx}&\mu_{zy}&\mu_{zz}\end{bmatrix},\quad \overline{\overline{\varepsilon}}_r=\begin{bmatrix}\varepsilon_{xx}&\varepsilon_{xy}&\varepsilon_{xz}\\ \varepsilon_{yx}&\varepsilon_{yy}&\varepsilon_{yz}\\ \varepsilon_{zx}&\varepsilon_{zy}&\varepsilon_{zz}\end{bmatrix} \quad (5)$$

The properties of lossy anisotropic media can be characterized by $\overline{\overline{\mu}}_r^{-1}$ and $\overline{\overline{\varepsilon}}_r$ in (4) if it is needed, which is easy to implement. For the isotropic media here, $\overline{\overline{\varepsilon}}_r$ and $\overline{\overline{\mu}}_r^{-1}$ are reduced to scalar ε_r and $1/\mu_r$, respectively.

For the fields matching on the interface areas S_j between the complicated junction space and regular waveguides, there exist the following equations:

$$e_{11}^{in}\vec{e}_{11}^{in}(x,y,z)+\sum_{l=1}^{L}e_{1l}^{s}\vec{e}_{1l}^{s}(x,y,z)=\sum_{n=1}^{N}A_n\vec{N}_n(x,y,z) \quad (6)$$

$$\sum_{l=1}^{L}e_{il}^{s}\vec{e}_{il}^{s}(x,y,z)=\sum_{n=1}^{N}A_n\vec{N}_n(x,y,z)\qquad i=2,3,4 \quad (7)$$

By multiplication crossing $\vec{h}_{jl}(x,y,z),\ l=1,2,\ldots,L$ on both sides of (6) and (7), and integrating over $S_j,\ j=1,2,3,4$, respectively, $4*L$ linear equations are gained. Where $\vec{h}_{il}(x,y,z)$ denotes magnetic vector eigenfunction of the lth mode in the ith waveguide. Then a matrix equation is obtained.

$$AX=B \quad (8)$$

Where

$$A = \begin{bmatrix} [\Gamma_{N\times N}[C]_{N\times 4L} \\ [D]_{4L\times N}\,\mathrm{diag}[T]_{4L} \end{bmatrix}_{(N+4L)\times(N+4L)} \tag{9a}$$

$$[\Gamma]_{ij} = \iiint\limits_{I} \left[\nabla\times\vec{N}_i\cdot\left(\overline{\overline{\mu}}_r^{-1}\nabla\times\vec{N}_j\right) - k^2\vec{N}_i\cdot\left(\overline{\overline{\varepsilon}}_r\vec{N}_j\right)\right]dV,$$
$$i = 1,2,\ldots,N; \quad j = 1,2,\ldots,N \tag{9b}$$

$$[C]_{i[(j-l)*L+k)]} = \iint\limits_{S_j} \vec{N}_i\cdot\left[\hat{n}\times\overline{\overline{\mu}}_r^{-1}\left(\nabla\times e^s_{jk}(x,y,z)\right)\right]dS,$$
$$i = 1,2,\ldots,N; \quad j = 1,2,3,4; \quad k = 1,2,\ldots,L \tag{9c}$$

$$[D]_{[(j-l)*L+k)]j} = \iint\limits_{S_i} \vec{N}_j\times[h^s_{ik}(x,y,z)]\,dS,$$
$$i = 1,2,3,4; \quad j = 1,2,\ldots,N; \quad k = 1,2,\ldots,L \tag{9d}$$

$$\mathrm{diag}\,[T]_{(i*L+k)} = \iint\limits_{S_i} \vec{e}^s_{ik}(x,y,z)\times\vec{h}^s_{ik}(x,y,z)dS,$$
$$i = 1,2,3,4; \quad k = 1,2,\ldots,N \tag{9e}$$

$$[B]_i = \begin{cases} \displaystyle\iint\limits_{S_j} \vec{N}_i\cdot\left[\hat{n}\times\overline{\overline{\mu}}_r^{-1}\left(\nabla\times\vec{e}^{in}_{11}(x,y,z)\right)\right]dS & i = 1,2,\ldots,N \\ \displaystyle\iint\limits_{S_i} \vec{e}^{in}_{11}(x,y,z)\times\vec{h}^{in}_{11}(x,y,z)dS & i = N+1 \\ 0 & i = N+1, N+2, \\ & \ldots, N+4*L \end{cases} \tag{9f}$$

X are unknowns to be solved, as shown in followings:

$$X = (A_1, A_2, \ldots, A_N, e^s_{11}, e^s_{12}, \ldots, e^s_{1L}, e^s_{21}, e^s_{22}, \ldots, e^s_{2L}, e^s_{31}, e^s_{32}, \ldots, e^s_{3L}, e^s_{41}, e^s_{42}, \ldots, e^s_{4L})^T \tag{9g}$$

Solving this equation can get the characteristics of the magic tee.

3. NUMERICAL RESULTS AND EXPERIMENTAL RESULTS

In order to see the convergence of the obtained numerical approximations to the true solution, magic tee is meshed with different maximum tetrahedral-element edge lengths, respectively. The

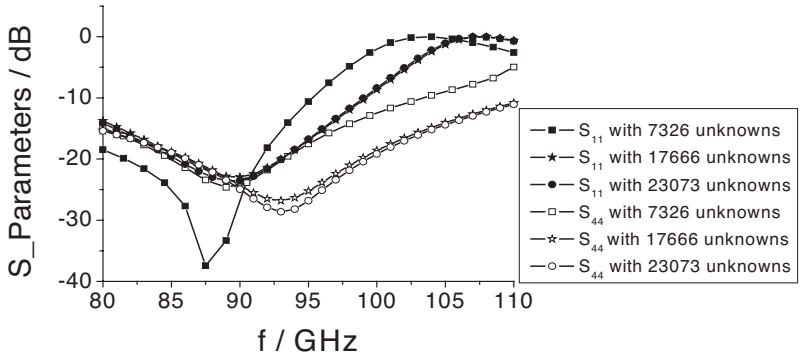

Figure 4. The convergence of the computation results.

comparison of the results with different unknowns is shown in Fig. 4. It can be seen from Fig. 4 that convergence of the numerical solution to equation (8) can be obtained when $N \geq 17600$ (maximum tetrahedral-element edge length is less than $\lambda/15$ in free space, λ is wavelength in free space.) In the following computation, the maximum tetrahedral-element edge length is set to meet the requirement above.

3.1. Performance of Magic Tee at W Band

The matching element in the junction of the magic tee in this paper is developed based on those in Fig. 1 and Fig. 2 except the matching metal steps or metal plates in port 4 are eliminated, as shown in Fig. 1 $\sim$ Fig. 3. In order to get good performance, a procedure of "try-and-error" for the different parameters of the matching element is carried out, which results in some numerical computation. After some numerical computation and getting good performance, magic tee was manufactured and experiments were carried out. Both the calculated results and experimental results are depicted in Fig. 5. Agreement can be seen. Without any matching components placed in the waveguide port 4 of the magic tee as shown in Fig. 3, the return loss below -20 dB for each port of the magic tee has a bandwidth about $8 \sim 9$ GHz. The isolation between port 1 and port 4, is below -30 dB in the band from 80 GHz to 105 GHz. The isolation between port 2 and port 3 also has a large bandwidth (about 18 GHz) in which S_{32} and S_{23} are below -20 dB. Because of some errors in the manufacture, there is some difference between the calculation results and measured results. For example, S_{41} and S_{14} calculated are much lower than those measured. The difference will be examined in following section.

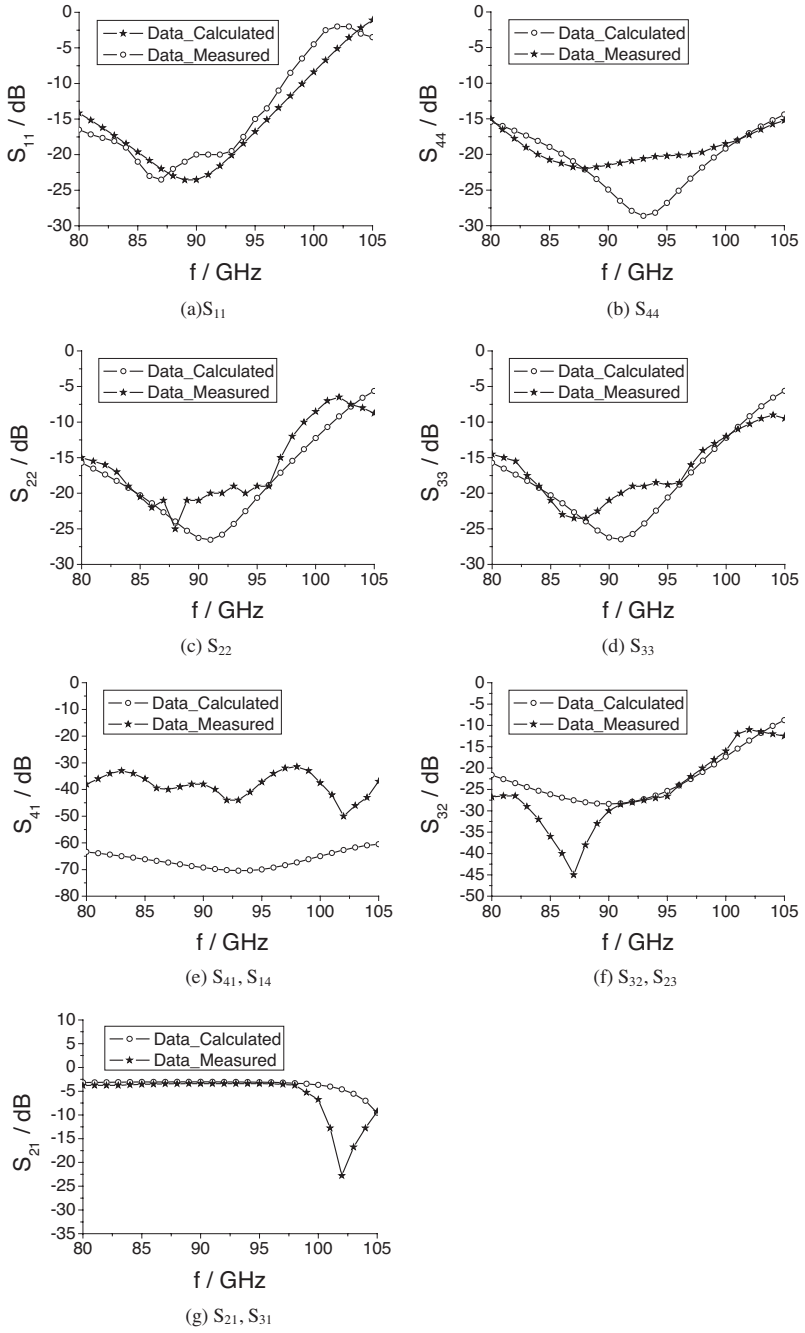

(a)S_{11} (b) S_{44}

(c) S_{22} (d) S_{33}

(e) S_{41}, S_{14} (f) S_{32}, S_{23}

(g) S_{21}, S_{31}

Figure 5. Performance of magic T-junction.

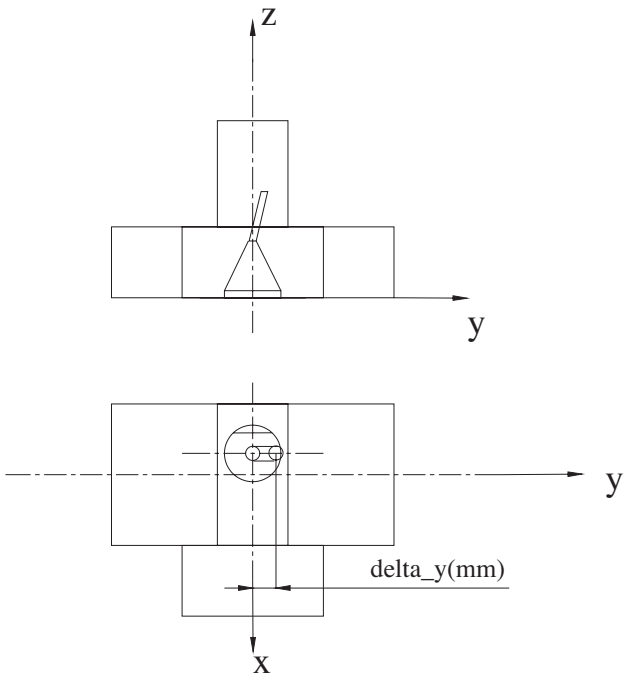

Figure 6. Schematic diagram of magic tee with the inclined thin pole of matching element.

3.2. Sensitivity Analysis

Fig. 5(e) shows an obvious difference between calculated result and measured result. We want to know the cause. So a sensitivity analysis is carried out. After much calculation, we find that little incline of thin pole matching element in y-axis direction can make S_{41} (and S_{14}) degrade very much, but other scattering parameters may keep almost same. For the case that the thin pole of matching element is inclined, as shown in Fig. 6, the calculation results are given in Fig. 7. It can be seen from Fig. 7 that the performance of S_{14} and S_{41} of the magic tee has been degraded from -60 dB to -40 dB if the thin pole has little incline along y-axis. Meantime, other scattering parameters stay almost the same as before. It should be pointed out, although the S_{14} or S_{41} has degraded from -60 dB to -40 dB, the absolute amount of changed is still very small. Hence the variance of other scattering parameters cannot be observed obviously. Therefore, it is believed that the difference between the calculated results and the

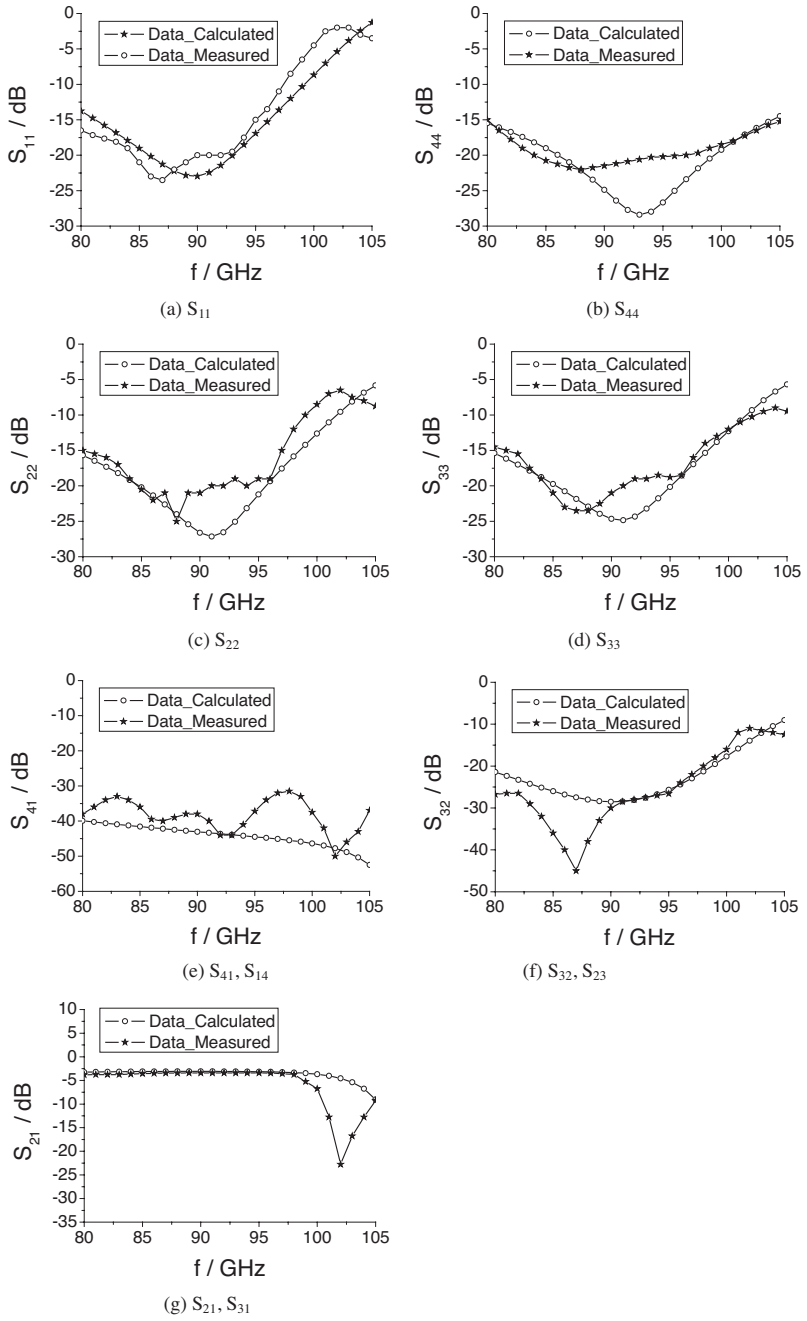

(a) S_{11} (b) S_{44}

(c) S_{22} (d) S_{33}

(e) S_{41}, S_{14} (f) S_{32}, S_{23}

(g) S_{21}, S_{31}

Figure 7. Performance of magic tee with delta_$y = 0.01$ mm.

experimental results on S_{14} and S_{41} shown in Fig. 5(e) comes from the little incline along y-axis of thin pole. Of course, other little tolerance of manufacture also exist, such as little variance of waveguide width or height, little warp between port 4 and port 1 and so on, which results in other difference between calculated and experimental results.

3.3. Evaluation of Power Carrying Capacity of the Designed Magic Tee

For TE_{10} mode, the transferring power of the waveguide can be expressed as:

$$P_{TE_{10}} = \frac{1}{2Z_{TE_{10}}} \int_0^a \int_0^b |E_y|^2 dxdy = \frac{abE_{10}^2}{4Z_{TE_{10}}} = \frac{abE_{10}^2}{480\pi} \sqrt{1 - \left(\frac{\lambda}{2a}\right)^2} \tag{10}$$

Here, a denotes the width of the waveguide, b denotes the height of the waveguide, and E_{10} denotes the magnitude of E_y at the center of the waveguide's width.

For the each case that electromagnetic wave input into magic tee from different ports respectively, the maximum E-field in the magic T-junction is calculated and presented in the Fig. 8. The maximum E-fields shown in the figure have been normalized to $e_{i1}^{in},\ i = 1, 2, 3, 4$, which is the amplitude of the input wave respectively. Because the maximum E-field in magic tee is about 6.5 times of input E-field, the power carrying capacity of magic tee reduces very much than the waveguide. We know the break down voltage of the air is 30 kV/cm, so the maximum power carrying capacity of the design magic tee is about 368 W.

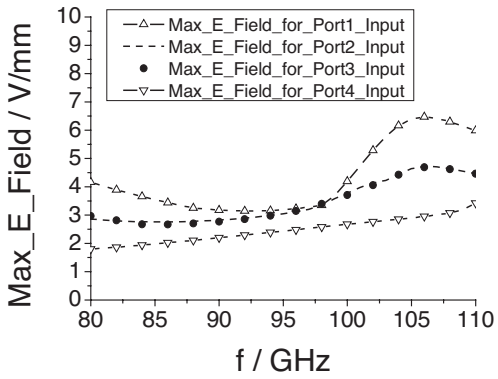

Figure 8. Maximum E-field in magic tee.

4. CONCLUSIONS

Waveguide magic tee at W band is analyzed by proposed method and developed. The computation results are compared to those in experiments, and agreement has been observed. Sensitivity analysis is carried out to show the influence of fabrication tolerance on the performance of the magic tee. It is believed that the difference between computation and experiments is from the little tolerance of manufacture. The magic tee designed has a structure that is convenient for manufacture and its good performance can meet the requirement of practical system. Finally, the power carrying capacity of the designed magic tee is also evaluated.

REFERENCES

1. Sieverding, T. and F. Arndt, "Modal analysis of the magic tee," *IEEE Microwave Guided Wave Lett.*, Vol. 3, 150–152, May 1993.
2. Ritter, J. and F. Arndt, "Efficient FDTD/matrix-pencil method for the full-wave scattering parameter analysis of waveguiding structures," *IEEE Trans. Microwave Theory Tech.*, Vol. 44, 2450–2456, Dec. 1996.
3. Shen, Z. X., C. L. Law, and C. Qian, "Hybrid finite-element-modal-expansion method for matched magic T-junction," *IEEE Trans. Magnetics*, Vol. 38, 385–388, March 2002.
4. Beyer, R. and U. Rosenberg, "CAD of magic tee with interior stepped post for high performance designs," *IEEE-MTTS International Microwave Symposium Digest*, Vol. 2, 1207–1210, June 2003.
5. Peterson, A. F. and S. P. Castillo, "A frequency-domain differential equation formulation for electromagnetic scattering from inhomogeneous cylinders," *IEEE Trans. Antenna Propag.*, Vol. 37, 601–607, May 1989.
6. Wu, H. and W. Dou, "Analysis of waveguide multi-ports discontinuities by the Helmholtz weak form and mode expansion," *IEE Proc.-Microw. Antennas Propag.*, Vol. 151, 530–536, Dec. 2004.
7. Stenger, E., M. Sarantos, E. Niehenke, H. Fudem, C. Schwerdt, F. Kuss, D. Strack, G. Hall, and J. Masti, "A miniature, MMIC one watt W-band solid-state transmitter," *IEEE-MTTS International Microwave Symposium Digest*, Vol. 2, 431–434, June 1997.
8. Jin, J. M., *The Finite element Method of Electromagnetism*, Xi'dian University Press, Xi'an, 2001 (in Chinese).